

PRELIMINARY REPORT ON THE TSUNAMI CAUSED BY SISSANO THE  
EARTHQUAKE AT, WEST SEPIK, PNG ON 17 JULY 1998

Yoshiaki Kawata\* · Yoshinobu Tsuji\*\* ·  
Hideo Matsutomi\*\*\* · Koji Fujima\*\*\*\* ·  
Fumihiko Imamura\*\*\*\*\* · Masashi Matsuyama\*\*\*\*\* ·  
Tomoyuki Takahashi\*\*\*\*\*

## ABSTRACT

The first investigation on the tsunami caused by the earthquake offshore north-western coast of the Papua New Guinea (PNG) was carried by the Tsunami Survey Team (ITST) during the period of 31 July to 7 August 1998. The survey to the aged area confirmed the 7-10 m wave reported and found the place where the waves were larger-up to 15 m and extreme overland flow velocities of 10 to 15 m/s. The severe damage and extreme wave heights were confined to a relatively short (30 km) stretch of coast between Aitape and Sissano Villages and specially large along the sandbar the outer margin of Sissano Lagoon.

## 1. INTRODUCTION

On the evening of Friday 17 July at around 7:30 pm a massive tsunami swept across the sandbar that forms the outer margin of Sissano Lagoon, west Sepik,

PNG. Initial media reported that the tsunami struck west of the town of Aitape in the west Sepik province, hitting at least four villages. And the wave was between 7 and 10 meters and that up to 3,000 persons were killed or missing. This seemed to be an unusually damaging tsunami given the size of the earthquake ( $M = 7$ ). Members of the International Tsunami Survey Team decided that a field survey was necessary as soon as possible to try and determine the true value of the maximum runup and to accurately map the runup distribution along the coast. Upon arrival at the disaster relief command post in Aitape, the team was granted full access to the sealed region around Sissano Lagoon and Sissano Village, the site of the most deaths and greatest destruction.

In the past six years, the international scientific community as responded to all previous nine major tsunami disasters (Nicaragua, 1992, Flores, 1992, Okushiri, 1993, East Java, 1994, Mindoro, 1994, Kuril islands, Russia 1994, Manzanillo, 1995, Irian Jaya, Indonesia, 1996, Peru, 1996) by dispatching a team of scientists which has come to be known as the International Tsunami Survey Team (ITST for short) (refer Yeh et al.:1993, Synolakis et al.:1995, and Imamura et al.:1997).

\* DPRI, Kyoto University  
\*\* ERI, Univ. Tokyo  
\*\*\* Akita Univ.  
\*\*\*\* National Defence Academy  
\*\*\*\*\* DCRC, Tohoku Univ.  
\*\*\*\*\* CRIEPI

More than thirty different colleagues and more than twenty different students have participated in these surveys, from Indonesia, Korea, Japan, Mexico, Peru, Russia, United Kingdom, and the United States. In the PNG survey, we were joined by colleagues from Australia and New Zealand.

## 2. SURVEY TEAM

The international tsunami community have conducted many field investigations immediately after an event: e.g. Nicaragua in 1992; Flores Island, Indonesia, in 1992; Okushiri Island, Japan, in 1993; East Java, Indonesia, in 1994; Shikotan Island, Russia, in 1994; Mindoro Island, Philippines in 1994; Irian Jaya, Indonesia, in 1996; Peru in 1996. Saving lives through improved hazard mitigation is the ultimate purpose of these surveys, and these improvements can be gained only through the collection of valuable data that lead to a better understanding of the tsunami phenomena. Unfortunately, these data are highly perishable (please see the 1998 IOC Post-Tsunami Survey Guide), and the survey must be conducted within a few weeks. But our community, through long experience, is highly aware of the human tragedy and the extremely sensitive nature of a post-disaster situation shortly after the event. In all cases, we seek government approval to conduct the survey, and always conduct a post-survey briefing and provide local officials with all survey results, which are valuable in planning recovery operations and developing effective mitigation policies. We also conduct the survey with local scientists, sharing our experience with them. During each tsunami event, *this process has served to increase*

the number of local scientists and emergency managers that actively participate in the larger tsunami hazard mitigation community.

The survey was conducted by a multinational team with representatives from Japan, the United States, Australia, and New Zealand. The team was broken up into two groups, the Japanese and everyone else. The Japanese team traveled overland from Wewak to Aitape measuring runup along the way. Japanese team members also installed seismograms in the region (Wewak, Lumi and Vanimo) to measure aftershock activity. The rest of the team traveled by ship from Wewak to the west stopping at some of the offshore islands. The two groups reunited in Aitape before a survey of the Sissano area was conducted. The boat continued west as far as Serai Village where runup values were seen to diminish considerably.

## 3. LOCATION OF AITAPE AND DAMAGE

### 3.1 Geographical Situation of Aitape and Sissano

After Sissano to east there was lagoon of Sissano where village of Warapu is located after Warapu followed the region of Arop and Malol. All these villages were situated along the coast. The two rivers of Arnold (Bliri) and Yalingi form the boundaries between the various regions. The hinterland behind the region is swampy right up to the foot of the terricelli mountains. These swamps are bounded near the coast of many other lagoons. The largest one belongs to the lake village of Warapu. The settlements there were built on the narrow strip of land lying between the sea and the lagoon. *The land which the*

villages used to build their houses on was slightly raised 1-3 meters above the sea level. The area was mostly surrounded by dense coconut trees. Coming closer to Aitape there is a change of the geographical scenery. Elevated coral formations were closer to the coast with people of cape Lapar. The live hood of the people was heavily depend on sea and the lagoon and they were very well know for their seamanship and their fishing expertise. They lived very happy lives and had a staple diet of fish and sago.

### 3.2 History of Aitape

Aitape is a tiny, picturesque town with evidence of its history. The Germans established their station here in 1905 and the jail they built in 1906 still stands above the town. It was used by the Japanese during the world war II.

The majority of the people were devote Catholics as the base of the early missionaries was in Aitape. Some of the parishes which were built before World War I were Malol (1908) and Sissano (1911). The church building at Sissano was swept into the lagoon by the tidal wave (tsunami) along with other buildings and village houses.

This was not the first time for a disaster has struck the area. In 1907 a similar tsunami caused by an earthquake hit the same area but did not claim as many people killed as the recent one had. There

was also another huge earthquake in 1935 but there were no tsunamis.

### 3.3 Recent hazards in PNG

Statistics show that 37 People died in the Finesttere Range between Madang and Lae in 1993 from landslide, an earthquake in Madang in 1970 killed 15, a 1979 earthquake in Port Moresby claimed no lives but cause massive damage, as did the twin volcanic eruptions in Rabaul in 1994, Mt Lamington blast. Having borne the brunt of a tidal wave back in 1907, when the population at the point of impact was apparently small. Aitape's residents should have been aware of the risk involved in living on the coastline.

### 3.4 Casualties

The death toll of the Aitape tsunami disaster has been confirmed at 2,182 as of 7 August 1998 while over 500 people are still missing. Major human damage are reported from three villages on sandbar of Sissano lagoon as shown in Table 1. The number of deaths is expected to rise further because many people are still unaccounted for with some bodies still in the lagoon.

## 4. TECTONICS AND THE EARTHQUAKE

### 4.1 Tectonics Backgrounds

The Papua New Guinea and neighbouring regions are bounded by latitudes 1-12 S and longitudes 130-163E. The earthquake

Table 1 Major casualties at three villages as of 7 August 1998

	Death	Injured	Survivors
Warupu	1,071	369	1,460
Arop	863	0	1,404
Malol	126	0	3,616

actively results from the collision of the major lithospheric plates Pacific and India-Australia, except at the extreme central west of the region where the furthest eastward extension of the Eurasia plate extends eastward beyond longitude of 130° E India-Australia/Pacific Plate collision.

Tectonics in Northern Sepik region is summarized as follows. The combination of the North Bismarck and (Caroline) Pacific plates north of the Bismarck sea seismic zone obliquely collide with the India-Australia Plate margin in the region north of the Sepik River. The Pacific Plate is underthrusting the margin, or subducting beneath it. The subduction is not the extension type, in which the ocean plate falls away in front of the margin. The Pacific plate is being obliquely driven into the continental margin. The thick 20 km crust of the Eapirik-New Gunear Rise (Den et al, 1971) may be inhibiting the subduction process. However Letz (1985) and Davies (1990) consider that the intermediate depth seismicity beneath the Sepik and central Irian Jaya to be associated with Pacific Plate subduction. The intense shallow seismicity north of the Sepik reflects the deformation of the overlying plate margin as it is dragged WSW by the underthrusting Pacific Plate. The Irian Jaya section of the Papuan Fold Belt seismic zone may represent the southern limit of westward drag on the India-Australia Plate.

#### 4.2 Earthquake of 17 July 1998

Several research institutes in the world provides quick solution of earthquake mechanism. All of them suggest shallowly or steeply dipping reversed fault with the magnitude of around 7, while a location of estimated epicenter varies from inland

to 50 km offshore.

From the seismological standpoint, this event baptized as the Sissano earthquake was only of moderate size. Estimates of its conventional magnitudes are  $m_b$  6.9 and  $M_s = 7.0$ . The seismic moment was determined by the Quick CMT algorithm at Harvard to be  $M_0 = 5.2 \times 10^{26}$  dyn-cm ( $M_w = 7.1$ ). Mantle magnitude estimates computed at Papeete and Northwestern University were  $M_m = 6.8$ . The slight discrepancy between body- and surface-wave magnitudes is upheld by the calculation of the estimated energy in the body waves, and of the slowness parameter  $Q = \log_{10}(E/M_0) = -5.5$ . This indicates that the earthquake source was somewhat deficient in high frequencies, but it did not exhibit the strong character of slowness found in "tsunami earthquakes", such as Nicaragua (1992;  $Q = -6.30$ ) or East Java (1994;  $Q = -6.01$ ) by Newman and Okal (1998). This is supported by the observation that the mantle magnitude of the earthquake is stable with frequency, and does not grow with period, as was the case for the tsunami earthquakes. The Sissano earthquake was followed 20 minutes later by an aftershock of  $m_b = 5.6$ . Careful study shows that the aftershock was itself preceded by a smaller event, 30 seconds earlier, with magnitude  $m_b = 5.3$ . The aftershock has a mantle magnitude  $M_m = 5.75$  and  $Q = -4.80$ , indicating that it was not a slow event.

The preliminary epicenter of the Sissano earthquake was given by the NEIC at 3.10S; 141.80E, a location significantly inland; however, this epicenter has now been revised to 2.932S; 141.797E which is practically on the coastline, 7 km to the West of the Serai lumber mill. The aftershock's location (2.916S; 142.081E) is at sea, 7 km due North of Sissano Lagoon.

The preliminary characteristics of the source of the earthquake, obtained by Japanese seismologists, suggested a fault area of 30 by 15 km, with a slip of about 2 m. This geometry would be in general agreement with a simple model in which the hypocenter of the main shock would be at the Western end of rupture, and the aftershock would mark the position of the Eastern end. The Harvard CMT mechanism can be interpreted either as shallow angle oblique subduction of the Caroline plate under the Sepik province, or as nearly pure dip-slip on a fault dipping steeply 79 NNE.

According to staff of the Port Moresby Geophysical Observatory, there were two strong earthquakes on that Friday evening, one at 6:49 pm and the other at 7:09 pm. The first had a magnitude of 7.0 and the second earthquake was probably slightly weaker. The latest best fix for the location of the epicenter of the first earthquake is 2.9 degrees south latitude and 141.8 degrees east longitude. This a point very close to the coast near the Serra Hills, 35 km west-northwest of Sissano. The location of the epicenter of the second earthquake was not determined.

The earthquakes were strongly felt. One of students of University of PNG who was at Aitape describes an undulating movement of the earth that was so strong that she and her friends lay on the ground to avoid falling over. The eyewitnesses obtained in this survey shows modified Mercalli Scale (MMS) ranging 5 to 7 which is strong ground shake corresponding to an earthquake with  $M = 7$ . This indicates that the event would not belong to slow earthquake, which is one of tsunami earthquake.

## 5. MEASURED TSUNAMI AND RESULT OF THE SURVEY

### 5.1 Logistics and Generalities

The objective of a tsunami survey is to measure inundation or flow depth heights and inland penetration distances, whenever watermarks and other indicators can be found. Most watermarks are highly ephemeral and they maybe lost only after a single storm. Earth-moving equipment may destroy the vegetation the ITST relies upon to infer the direction and size of the tsunami currents. Eyewitnesses usually move to safer areas or they are relocated, and sometimes may not welcome being tracked down months later to discuss what may well have been the most painful experience of their lives. Quite frequently, once an official version of an event circulates, all eyewitnesses report identical information, as it is in human nature for people to trust what they hear or read from the press instead of their own eyes. When this type of information is lost, it becomes much more difficult than already is to reconstruct the event.

IOC (1998) summaries the methodology to measure a runup height and maximum water level referring objects, traces and markings. Inundation heights above sea level were estimated based on clear tsunami effects, such as tsunami runup, and interviews with eyewitnesses. Tsunami runup indicators used in this survey included marks on walls and windows left by dirty water, the boundaries of areas where salt water had killed vegetation or where water had carried debris, and places where eyewitnesses could identify the limit of inundation or clearly remember how deep the water had been, for example, up to the top of a tree. The measurements were



subject to errors of up to several tens of centimeters, generally within 10 % error of the measured data.

Inundation surveys involve measuring tsunami inundation height and inland penetration distances, whenever watermarks and other indicators can be found. This data is highly ephemeral and maybe lost even after a single heavy storm. Whenever possible, the team also measures aftershock distributions to better determine the rupture area. The ITST uses standard surveying gear, GPS computers for locating the inundation marks consistently on maps, corers for sediment sampling and portable seismometers.

## 5.2 Survey Result

Sissano lagoon is fronted on the ocean side by a sand bar with a fairly narrow mouth. The lagoon is almost semicircular with its back side distant about 4 km from the mouth; as seen in figure 1 and photograph 1. At its eastern end there is the village of Arop with the village of Sissano about 1 km west from the lagoon entrance. There was no evidence of any of houses or their remains anywhere along the bar, other than bent 2×2 stilts which were used in their foundations and which were normally vertical. Many of the remaining coconut trees which had not been swept away far into the lagoon were bent close to the roots or had been uprooted. (Photographs 2 and 3.) The average flow depth over the sandbar near the lagoon mouth was 10 m, while near Arop it reached 15 m. Note that it was not possible to determine maximum runup, since the most land ward penetration point was over 4 km away in a swamp where crocodiles had been reported. The team inferred that the

water current induced by the tsunami over the peninsula was at least 10m/s or about and most probably it peaked to twice this value; these estimates are consistent with local eyewitness reports whose descriptions allowed local scientists to infer 15-20m/s current velocities. It should be noted that the force of the tsunami current on an object is 1000 times greater than the force on the same object by a wind of the same speed. The team also observed sediment deposition of up to 15 cm, and evidence of scour and sediment splays. Three team members sailed with a smaller boat inside the lagoon in an attempt to determine how far the wave had penetrated. Navigation was difficult because of the number of entire trees, tree-stumps and building debris that were scattered everywhere, and it was not possible to reach to the back of the lagoon, about 4km away, without significant further danger to team members. However, they did notice that the debris from the community on the sand bar reached to the back of the lagoon which is swampy and fronted by mangroves. The height of the wave there was probably less than 1m, as there were at least a few houses on stilts still standing.

## 5.3 Distribution of Tsunami Runup Heights

In total, 80 inundation data point were measured and 30 different topographic transects, covering densely an area of more than 40 km, with several additional points measured at Vanimo (about 100 km west of Sissano) and Wewak (180 km east). Generally, as seen in figure 2, the inundation heights diminished rapidly about 10 km east and west from the

worst hit area which extended between Arop and Sissano. At the village of Serai, about 15 km from the lagoon mouth, the inundation height was about 4 m, and there was no damage to the village. The coastal topography changed suddenly at about 7km west of Serai, where measurements in a lumber mill suggested a 1.5 m runup height. There were no reports or observations of damage beyond that point, yet the tsunami was observed by eyewitnesses in Wutung, Vanimo and in Manus

island and recorded by tidal gage stations in Japan and Hawaii. In Wutung, on the border with Indonesia the wave height ranged from 2 m-3 m. No evidence could be found on the surveyed shores of permanent deformation associated with the earthquake itself, nor did any eyewitness indicate permanent changes in sea level, the only exception to this pattern being a rock slide in a strongly weathered cliff at the Serai lumber mill, and an instance of liquefaction documented at Arop.

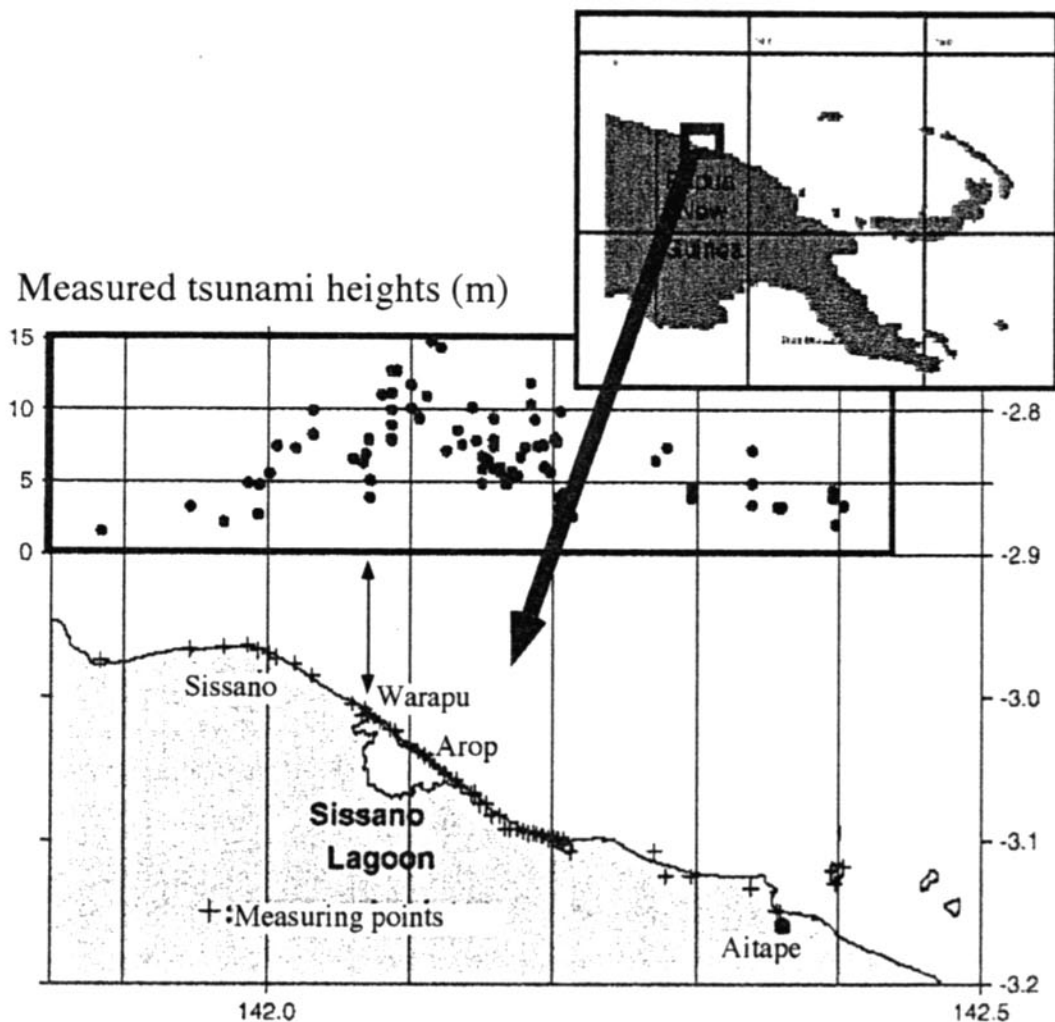


Figure 1 Measured tsunami heights along the coastal line. All data are corrected to be value at the time of the tsunami attacked by modifying the tidal components.

#### 5.4 Tsunami observed at each region (a) Sissano Lagoon

The average maximum heights of the tsunami waves they crossed the Sissano sandbar was about 10 meters. The wave heights were determined by the team, using tsunami traces and marks such as damaged to the front of coconut plams.

However, the wave height varies at different points long the sandbar and was as high as 15 m above the sea level at the former site of the Arop village. In this 1.2 km long sector of the sandbar long sector of the sandbar nothing was left standing now. There was a complete stripping of structures and trees.

Several lines of evidence point to an origin of the tsunami near Sissano. The best evidence is the extreme wave heights recorded on the Arop sector of the lagoon sandbar.

Another piece of evidence is that damage to structures at the mouth of the Bliri river, west of Sissano, was clearly infected by a sea wave that was travelling westward.

The maximum energy of the tsunami seems to have been narrowly focussed on to a 40 km strip of coastline between the Bliri river and Aitape, and the energy to have falled away rapidly to either side of this strip. The narrow focus of the tsunami energy is surprising.

It is clear that most of the tsunami seems to be failry narrowly focussed on a 40 km strip of coastaine between the Arnold (a.k.a. Piore, Bliri) river and Aitape, and diminished rapidly to either side. This narrow focus of the tsunami energy is surprising. The wave appears to have moved from the east near the Bliri river, but when attacking the narrow sandbar off Sissano lagoon it propogated practically *perpendicular to the shore, suggesting*

that it spread radially from a source almost directly off Sissano and then dissipated rapidly. The first wave arrived within five to ten minutes from the mainshock and was reported uniformly as a leading depression N-wave (LDN). The elevation wave following was reported as a wall of water with thunder resembling the noise from jet aircraft and one person described the wave as C-shaped from an angle, suggesting a plunging breaker. The first wave was followed shortly thereafter by another two waves, the third of which was clearly smaller than the first two. It appears that all waves were closely spaced in time, suggestive of a highly dispersive wave train, rather than individual waves generated by strong aftershocks or sequential rupture.

#### (b) Wutung

The effect of the first sea wave were seen as far west at Wutung, on the border with Indonesia, and probably extended into Irian Jaya. Around Wutung, the wave ranges a heights of between two and three meters different locations. The wave arrived at Wutung at the same time the second earthquake. This is about the delay that one would expect for a wave originating near Sissano In the opposite direction, a sea wave less than a meter high recorded Wewak.

## 6. DISCUSSIONS ON THE TSUNAMI

### 6.1 Tsunami Magnitude

Prof. K. Abe tentatively estimated the tsunami magnitude  $M_t$  for the July 17 Papua New Guinea tsunami from tsunami wave amplitudes recorded in Japan Used formula

$$M_t = \log H + B$$

*H: Average of maximum tsunami ampli-*



tudes re-corded in Japan

B: Constant which depends on each pair of source region and observation region

For the source region south of Japan,  $B = 8.4$ . This value has been obtained for the Guam and Mariana events and has not yet been published. (Cf. Abe, K., J. Geophys. Res., 84, 1561, 1979)

Data Eleven data are available throughout Japan.  $H(\text{average}) = 0.13$  meters  $\pm 0.03$  meters. Result  $M_s = 7.51$ . USGS obtained  $M_s = 7.0$  from seismic surface waves.  $M_s$  is greater than  $M_w$  by 0.5. The PNG event is considered to be a tsunami earthquake that generates significantly large tsunamis but relatively weak seismic waves.

## 6.2 Location of tsunami source

We had carried out a field survey along the coast from Sissano Village to Aitape (see <http://www.tsunami.civil.tohoku.ac.jp/hokusai/2/news/PNG-result.htm>). Measured water level which indicates the scale of this tsunami was 10 meters and the maximum was 15 meters. This was too bigger than tsunamis caused by earthquakes of magnitude 7. Second feature is that the tsunami arrived very small region. The coastline where water level exceeded 5 meters was 40 km length and the heights exceeded 10 meters along only 20 km coast. Therefore, the huge tsunami attacked very local area.

Because this tsunami generated a catastrophic damage as compared with the magnitude of the earthquake, a slow earthquake was supposed. But differences between  $M_s$  and  $M_w$  presented by some institutes are small and the supposition is denied. We can image a submarine landslide as a factor of the huge tsunami, and we need to study about bathymetry changes. Another factor is that the tsunami source

was close to the shore. The tsunami arrived the shore before tsunami energy had not dispersed enough, so the energy concentrated at the short coast. Locations of an epicenter presented by some institutes (table 2 and see <http://omzg.sccc.ru/tsulab/so19980717.html>) confirm this factor. Therefore, this event indicates that earthquakes close to shores can generate huge tsunamis even if magnitudes are not large. The reason of short distance between the shore and the earthquake is that a plate boundary is close to land. So the regions where plate boundaries locate near land have high tsunami risks potentially.

This earthquake occurred in or near a plate boundary, but its mechanism might be an inner plate type. Fault models given by some institutes are shown in table 2. All models has two type faults. They are a low dip angle fault which indicates a plate boundary earthquake and a high dip angle fault which indicates an inner plate earthquake. Former type faults of each models are different, however, all models have good agreement about latter type fault. Furthermore, a comparison between tide records and computed by Tanioka (see <http://corona.pmel.noaa.gov/~tsunami/PNG/>), and a pattern of stress descent by Kikuchi (see [http://www.eic.eri.u-tokyo.ac.jp/EIC/EIC\\_News/980717.html](http://www.eic.eri.u-tokyo.ac.jp/EIC/EIC_News/980717.html), in Japanese) suggest the high dip angle fault.

If this earthquake was the inner plate type, it can not be included in earthquakes which occurs periodically. And there is a risk that a plate boundary type earthquake will be generated in the near future. Same case was occurred in Japan. In 1994, an earthquake of  $M_w$  8.3 happened off the East coast of Hokkaido and made a large tsunami which had 10 meter runup heights. In the same area, another earthquake of  $M$  7.4 was

Table 2 Magnitude and Epicenter of the earthquake.

	Ms	Mw	Epicenter
ERI	7.0	6.9	(3.10S, 141.80E)
Harvard	7.0	7.1	(2.78S, 142.57E)
NEIC	7.0	7.1	(3.08S, 141.76E)

Table 3 Fault models of the earthquake.

	Strike	Dip	Slip
ERI	126	14	105
	291	77	86
Harvard	147	14	124
	292	79	82
NEIC	182	5	152
	299	88	86
Kikuchi	53	6	24
	299	88	95

also occurred in 1969. An interval of the two events was only 25 years. This reason was that the 1994 earthquake was the inner plate type and was not one of the periodic events. We can not deny that such case will occur off the North-West coast of Papua New Guinea. Therefore, we need to investigate seismicity continually in this area.

According to earthquake research experts in Tokyo the tsunami probably was caused by abrupt movement on a fault that displaced the sea floor. Their modeling showed that two meters of vertical displacement of the sea bed along a fault 18 km long would be required. For the time being we can accept this as the most likely cause of the tsunami. Movement on a fault at a point located somewhere near Serra Hills and at a depth of some kilometres below the earth's surface caused a magnitude 7.0 earthquake.

The same movement caused a rupturing of the sea floor along the surface trace of the fault. The movement of the sea floor,

in turn, displaced a large volume of sea water and thus produced a tsunami. The story will doubtless be refined over the coming weeks as more data are assembled. There are a number of outstanding questions. For example, if the epicenter were near Serra Hills why was the tsunami most severe at Sissano, 35 km further along the coast.

Another strange aspect is the delay of 20-30 minutes between the earthquake and the arrival of the tsunami. From my admittedly very limited knowledge of tsunamis, I would have thought the tsunami should follow within minutes of the earthquake.

An alternative explanation is that the tsunami was caused by a major submarine landslide. The sea bed offshore from Sissano falls away to a trench that is about 3.5 km deep. As the illustration shows, the inner slope of the trench up to the coast at Sissano, is relatively steep and is broken by a number of faults.

The earthquake would tend to establish unconsolidated sediments on the upper part of the slope offshore from Sissano and could cause them to slump seawards. If the slump were on a large enough scale it would cause a tsunami. Beneath the Aitape coastal-line and extending beneath the offshore slope seaward to the New Gunear Trench are packets of sedimentary rock separated by faults.

### 6.3 Magnitude of Tsunami Source Estimated by the Linear Theory

The important characteristics of the observed tsunami heights are: (1) The tsunami heights are very high in the region between Arop village and the inlet of Sissano Lagoon; the averaged tsunami height in this region is about 10m. (2)

The region where the averaged tsunami height is higher than 5 m (half of maximum height) is very narrow; the length of this region is about 30 km.

These suggest that the tsunami energy is concentrated in this narrow region. It is well known that tsunami energy is concentrated in V-shaped bay, peninsula, island, ridge and so on. However, contour lines of water depth off the damaged area are almost parallel, thus the concentration of tsunami energy in this event is not caused by bottom topography, but initial tsunami profile. In this section, initial tsunami profile is estimated by using Fujima's theory (Fundamental study on tsunamis generated on a shelf, Fujima et al., Proceedings of JSCE, in Japanese, in submit). In the theory of Fujima et al., coastline is assumed to be straight and beach slope is to be uniform, then tsunami propagation from two-dimensional arbitrary tsunami source can be estimated as a series solution of the linear long wave theory. Although simplified topography must be assumed to get a theoretical solution, Fujima's theory has the following advantages;

(i) An arbitrary 2D profile of initial water elevation is set for the problem.

(ii) The obtained solution is not affected by numerical errors.

(iii) The distribution of tsunami height along coastline is obtained easily.

On the other hand, when a numerical simulation is adopted for analysis, exact bottom topography is taken into account. However, small grid should be used to get the accurate result. Thus, large computation time may be required for a numerical simulation. In order to evaluate the effect of tsunami source profile, various tsunami source profiles should be checked. Then Fujima's method is effective in such a

fundamental study. At the present, about 30 cases of initial tsunami profiles were examined through Fujima's theory by varying several parameters. As a result, it becomes clear that the initial tsunami profile as shown in Fig.2 reproduces the observed distribution of tsunami height well. Length and width of tsunami source area are 40 km and 20 km, respectively. Maximum deviation of water surface from mean sea level is -2.5 m. A minus sign indicates the depression of water surface. And location of maximum deviation point is 20 km off the Sissano Lagoon. Estimated tsunami height distribution is shown in Fig.3

It should be noted that a part of tsunami energy might propagate toward offshore direction, in the actual phenomena. In fact, tsunami with the amplitude of 10 cm was recorded at Ogasawara Islands, Japan. In Fujima's theory, wave propagating toward offshore is refracted and reach the coastline, thus the evaluated tsunami height may tend to be overestimated. Energy propagating toward offshore is less than half of total energy. Therefore, if the actual bottom topography is taken into account in the analysis, the true value of maximum initial water elevation to reproduce the observed tsunami heights might be -2.5 m to -5 m. According to the analysis of seismograms, it was reported that the dislocation area was 40 km  $\times$  15 km, and subsided height was 1.8 m. Both length and width of tsunami source seem to agree with the results of the present examinations, however the subsided height expected from seismograms, 1.8 m, cannot explain the observed tsunami heights. Of course, because the present analysis is based on the linear theory, nonlinear effects are not considered in the present exami-

nations. If soliton fission is occurred, it is possible that tsunami height increases remarkably. However, in the present case, source area is close to the coastline and shelf is not so long, thus the generation of soliton fission seems so unrealistic.

Therefore, it is concluded that the maximum deviation of initial water elevation in harmony with the observed tsunami heights is  $-2.5$  m to  $-5$  m. The usual tectonic movement is difficult to generate the tsunami with the amplitude of 10 m.

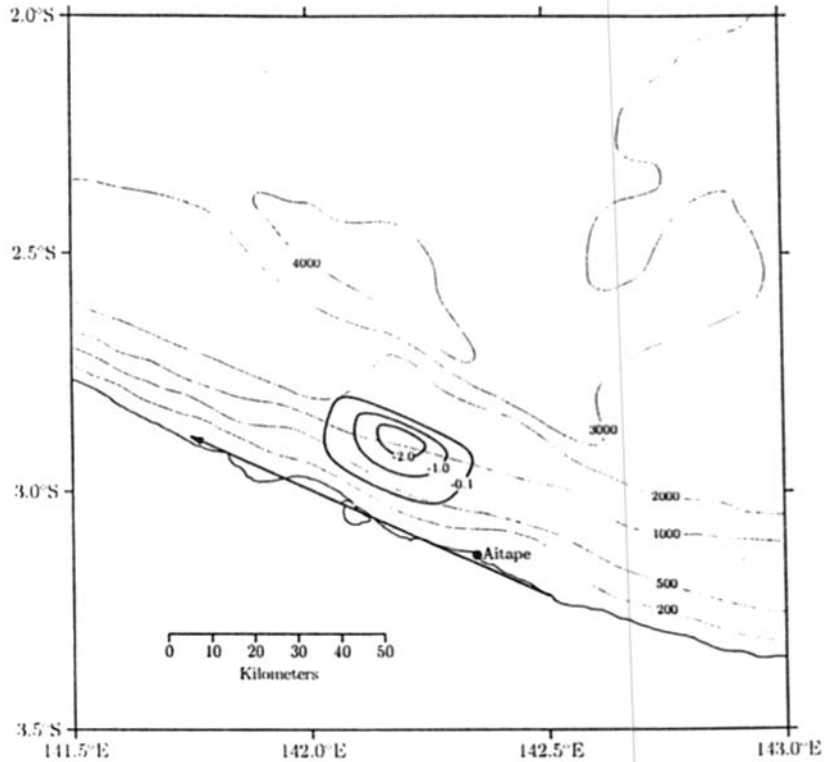


Figure 2 Assumed initial condition of the tsunami caused by a submarine landslide

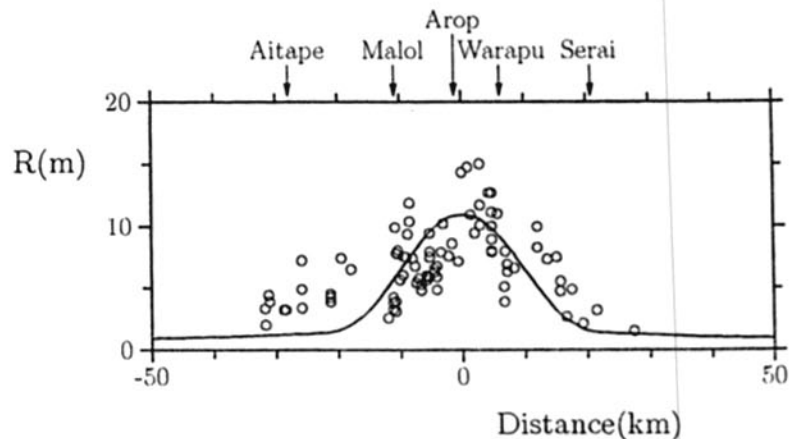


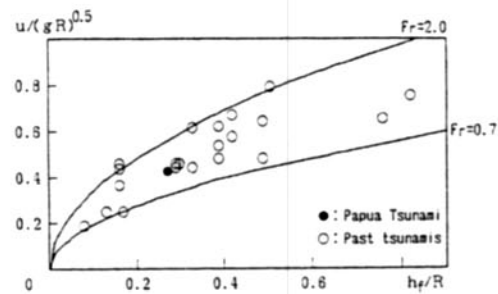
Figure 3 Comparison between theoretical and measured tsunami heights

## 7. HYDRAULIC PROPERTIES OF TSUNAMI

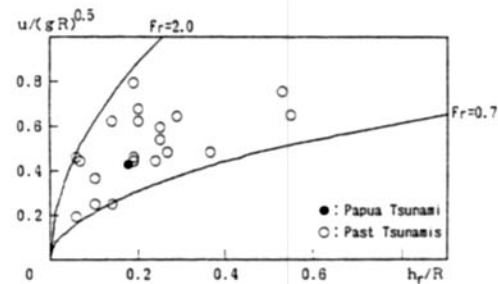
### 7.1 Relation between Inundation Depth and Current Velocity at Malol

There are relatively many data on inundation depth in regions where a tsunami countermeasure should be taken into consideration. Besides, nowadays, if an initial wave profile in a source region is given, the inundation depth at each coast is fairly accurately estimated by the conventional numerical simulation model. Hence, if a relation between the inundation depth and current velocity on land are clarified, fluid force on structures, moving velocity and impulsive force of floating bodies, strength of houses for tsunamis and so on, i.e., tsunami damages could be quantitatively discussed. In pursuit of realizing the above mentioned, the team has been collecting field data on the inundation depth and the current velocity.

Figures 4 (a) and (b) show the relation between the inundation depth  $h$  and the current velocity  $u$ . They are nondimensionalized by the gravitational acceleration  $g$  and the nearest runup height  $R$  to universalize the relation and to compare experimental data with the field data, and the subscripts  $f$  and  $r$  distinguish between front and rear sides of house. The difference between Figs. 4 (a) and (b) is that the front depth  $h_f$  and rear depth  $h_r$  of house are adopted as the inundation depth, respectively. The filled circles are data collected from the Papua New Guinea tsunami, and the open circles are data collected from past tsunamis (the 1992 Flores Island tsunami, the 1993 Hokkaido Nansei-oki tsunami, the 1994 East Java tsunami, 1996 Irian Jaya tsunami). The details of the data are shown in Table 4. These data were collected where



(a) Case by using depth



(b) Case by using rear depth

Fig. 4 Relation between non-dimensionalized inundation depth and current velocity.

the ground is almost flat or the ground height is a little higher than that in the surroundings, i.e., the seawater is not prone to remain on land. From the figures, it is clear that the data from the Papua New Guinea tsunami has the same tendency as that from the past tsunamis.

By the way, the current velocity is estimated by judging the inundation depths from tsunami traces on the front and rear walls of house and then applying them to the Bernoulli's theorem. As tsunamis are generally long waves, this method seems to be acceptable. The theorem on a horizontal bed can be expressed as

$$h_f = u^2 / 2g + h_r \quad \dots\dots(1)$$

where  $u$  is the depth-averaged current velocity in a main flow at a side of the rear



Table 4 List of inundation depths, current velocities and other remarks.

Location	Depth (m)		$\Delta h$ (m)	u (m/s)	Fr	R (m)	Plane shape of house	House type	Sym.	Remarks	
	$h_r$	$h$									
Wuring (Mosque)	1.56	0.91	0.65	3.57	1.2	3.19	Square (17.7×17.7m)	Brick	○	Side wall	
	1.56	1.19	0.37	2.69	0.8	3.19	" "	" "	○		
Monai	1.29	1.00	0.29	2.38	0.8	16.2	Rect. (7×12m)	Wood	○		
Inaho	4.45	1.70	2.75	7.34	1.8	8.81	Hexagon(15.6×19.0m)	R.C.	○		
Inaho elementary school	1.60	0.65	0.95	4.32	1.7	9.79	Rect. (36.3×29.3m)	Wood	○	Seaward Middle Landward	
	1.60	0.55	1.05	4.54	2.0	9.79	" "	" "	○		
	1.60	0.94	0.66	3.60	1.2	9.79	" "	" "	○		
Esashi	0.94	0.67	0.27	2.30	0.9	2.85	Rect. (14.5×48.0m)	R.C.	○	At ebb	
Pancer	1	1.60	1.30	0.30	2.42	0.7	9.40	Rect. (8.2×5.9m)	Brick	○	
	2	2.70	1.80	0.90	4.20	1.0	9.40	Rect. (12.8×5.3m)	Brick	○	
	3	1.21	0.91	0.30	2.42	0.8	9.40	H shaped(15.0×9.0m)	Brick	○	
	4	2.80	1.80	1.00	4.43	1.1	9.40	Rect. (10.2×19.2m)	Brick	○	
Lampon	1	1.58	1.02	0.56	3.31	1.1	5.40	Rect. (10.6×6.0m)	Brick	○	
	2	1.80	0.75	1.05	4.54	1.7	5.40	Rect. (8.9×10.0m)	Brick	○	
Korim	1	2.26	1.34	0.92	4.25	1.2	5.35	Rect. (15.0×14.0m)	Block	○	
	2	2.10	1.33	0.77	3.88	1.1	5.35	Rect. (30.2×10.5m)	Block	○	
	3	2.10	1.07	1.03	4.49	1.4	5.35	Rect. (18.0×7.6m)	Block	○	
	4	2.27	1.07	1.20	4.86	1.5	5.35	Rect. (27.0×7.3m)	Block	○	
	5	2.08	1.46	0.62	3.49	0.9	5.35	Rect. (14×7m)	Block	○	
Mansoben	2.43	1.58	0.85	4.08	1.0	2.98	Rect. (15.2×12.1m)	Block	○		
Pai Is.	2.22	1.60	0.62	3.49	0.9	2.92	Rect. (8.2×6.0m)	Block	○		
Malol	1.14	0.75	0.39	2.76	1.0	4.25	Rect. (15.0×10.6m)	Wood	●		

wall, and let us call this velocity Bernoulli velocity hereafter. Hence, the Bernoulli velocity is given as

$$u = \{2g(h_r - h)\}^{0.5} \quad \dots\dots(2)$$

Equation (1) is also rewritten as

$$h_r/h = Fr^2/2 + 1 \quad \dots\dots(3)$$

where  $Fr = u/(gh_r)^{0.5}$  is the Froude number. Up to date, the maximum values of  $h_r/h$  and  $Fr$  in the field data are 2.9 and 2, respectively (see Table 4). Substituting Eq.(3) into Eq.(2), an estimation equation of the current velocity in case of no energy loss is obtained as

$$u/(gR)^{0.5} = \{2Fr^2/(Fr^2 + 2)\}^{0.5} (h_r/R)^{0.5} \quad \dots\dots(4a)$$

$$u/(gR)^{0.5} = Fr(h_r/R)^{0.5} \quad \dots\dots(4b)$$

Equations (4a) and (4b) indicate that the current velocity on land is a function of the Froude number and is proportional to the square root of inundation depth. The latter agrees with a deduction from the long wave theory.

As seen from the above method, Eqs. (4a) and (4b) would be applicable only to a quasi-steady flow on land. The solid lines in Figs.1 (a) and (b) are Eqs. (4a) and (4b) for two different values of  $Fr$  and are envelopes for the field data. The envelopes on the upper side, which is the danger side for structures, are expressed as

$$u/(gR)^{0.5} = 1.1(h_r/R)^{0.5} \quad \dots\dots(5a)$$

$$u/(gR)^{0.5} = 2.0(h_r/R)^{0.5} \quad \dots\dots(5b)$$

At the present stage, Eqs. (5a) and (5b) would be recommended for practical use. Let us try to derive regression formulas in dimensional form from all the data for rough estimation of the current velocities in Section 3. The resultant formulas are expressed as

$$u = 2.6h_r^{0.7} \quad \dots\dots(6a)$$

$$u = 3.8h_r^{0.9} \quad \dots\dots(6b)$$

## 7.2 Relation between Inundation Depth and Degree of Damage to Houses

*Let us discuss with the relation between*

the inundation depth and the degree of damage to houses. Even if the inundation depth is the same, fluid force on houses depends on the Froude number (see Eq. (4b)) and places where the seawater is prone to remain or not. When the degree of damage to houses is discussed by the inundation depth, at least, it is necessary to distinguish between the places. Besides, the degree of damage to houses depends on types of houses. Discussion of it must be done for each type of houses. In the survey, only data of wood house (church) built on flat land at Malol was collected. Figure 5 shows the relation between the inundation depth and the degree of damage to houses. The front depth is adopted as the inundation depth. The degree of damage to houses is classified into three categories:

Destroyed (D.): walls are damaged and most of pillars are damaged. Restoration is not possible.

Partially Damaged (P.D.): pillars withstand, but a part of walls are damaged. Restoration is possible.

Withstood (W.): windows are broken, but pillars and walls withstand. It is possible to reuse with a slight repair.

The squares, triangles and circles mean destroyed, partially damaged and withstood, respectively. The filled data is collected from the Papua New Guinea tsunami and the open data are collected from past tsunamis in Japan. For your information, the houses are partially damaged at only 0.25 m inundation depth, which is due to collision of floating bodies. The house in Papua New Guinea is destroyed when the inundation depth exceeds 1.1 m. On the other hand, the depth is 2 m in Japan.

### 7.3 Relation between Sand Erosion Depth and Current Velocity

Recently, studies on sediment transport

due to tsunamis were begun to do, based on laboratory and numerical experiments. It would be useful to examine a relation between the erosion depth of sandy beach and the current velocity with field data.

Figure 6 shows the relation between the erosion depth  $h_s$  and the current velocity  $u$ . The definition of the erosion depth is shown in Fig. 7. These data were collected in a backshore region of sandy beaches. No information on sand grain size is obtained. The current velocity is estimated by judging the inundation depth from tsunami traces on coconut or other trees near the backshore region and then applying the depth to Eq. (6b). The filled circles are data collected

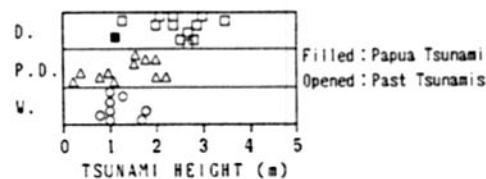


Fig.5 Relation between inundation depth and degree of damage to houses.

(Circles : withstand, Triangles : partially damaged, Squares : destroyed).

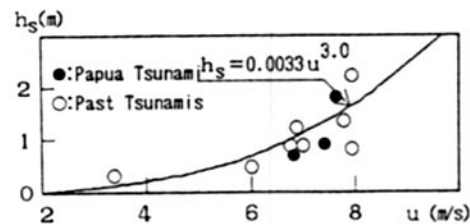


Fig. 6 Relation between sand erosion depth and current velocity.

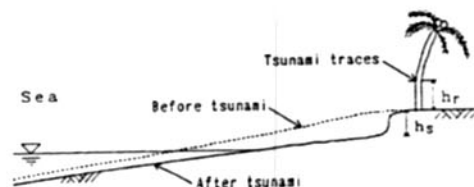


Fig. 7 Definition sketch of erosion depth.

from the Papua New Guinea tsunami. The open circles are data collected from the Flores, the East Java and Irian Jaya tsunamis. The solid line is a regression curve for the data, and it is expressed as  $h_s = 0.0033u^3$  (unit: m, s) .....(7) Equation (7) is a temporary yet because of the lacks of data and of the expression with dimensions. Figure 6 indicates that the sand erosion depth is proportional to the cube of the current velocity.

Next, let us roughly estimate the dependency of sediment discharge rate on the current velocity. The continuity equation of sediment is expressed as

$$\frac{\partial z}{\partial t} = - \frac{\partial q_B}{\partial x} (1-\lambda) \quad \dots\dots(8)$$

where  $z$  is the ground height,  $t$  is the time,  $q_B$  is the sediment discharge rate,  $x$  is the distance coordinate and  $\lambda$  is the porosity of sediment. Assuming that  $n$  waves attacked on a coast and the erosion depth resulted in  $h_s$ , Eq. (8) could be rewritten as

$$h_s = \int_0^{nT} \frac{dq_B}{dx} dt = \frac{d(\int_0^{nT} q_B dt)}{dx} = nT \frac{dq_{Bm}}{dx} \quad \dots\dots(9)$$

where  $T$  is the wave period and  $q_{Bm}$  is the time-averaged sediment discharge rate. Equation (9) is rewritten as

$$\begin{aligned} \frac{dq_B}{dx} &= \frac{h_s}{nT} = \frac{h_s L}{LnT} = \frac{h_s c}{nL} = \frac{h_s u}{nL} \\ &= \frac{h_s}{n} \frac{\partial u}{\partial x} = \frac{u^3}{n} \frac{\partial u}{\partial x} = \frac{\partial u^4}{\partial x} \quad \dots\dots(10) \end{aligned}$$

where  $L$  is the wave length and  $c$  is the wave celerity. Equation (10) indicates that the time-averaged sediment discharge rate due to tsunamis is proportional to the fourth power of the current velocity.

## 8. PRELIMINARY RECOMMENDATIONS.

- 1) There should be no relocation of people in locales which are fronted by water and backed by rivers or lagoons. Memorials should be built at the worst stricken locales to remind future inhabitants of this disaster and thus discourage future habitation of high risk locales. These memorials could be as simple as large signs.
- 2) Schools, churches and other critical facilities should never be located closer than 400 m from the coastline, and preferably 800 m in at-risk areas.
- 3) The local casuarina tree species withstands the wave attack significantly better than coconut trees, and casuarina forests should be planted in front of coastal communities, whenever possible.
- 4) There should be evacuation drills annually on the anniversary of this disaster so that all people in at-risk areas know that if they feel the ground moving they should run as far from the beach as possible.
- 5) Every family in an at-risk area should have a designated casuarina tree with a ladder or carved steps to allow vertical evacuation of the able, when there is no other option.
- 6) The residents in nonaffected areas should return to their homes, after being briefed about what to do in the event that they feel a ground motion or if they see unusual water movements. (As in most other 1992-98 tsunamis, this tsunami was preceded by an LDN, i.e., a leading-depression N-wave.)
- 7) The local fishermen should be allowed to resume fishing in the open ocean only. The local authorities should collect samples of the lagoon water (as described to

*them) and have them tested monthly to*

quantify the evolution of the water quality in the lagoon to determine when it would be safe again for fishing and habitation.

#### Future Prevention Work and Suggestions

Further work will continue to model the source and determine whether the possibility for a transpacific tsunami exists, either from the seafloor displacement or from a coseismic slump. It is hoped that a bathymetric survey will take place in the near future to attempt to find any evidence of slumping. (Interestingly, an NSF funded workshop in Santa Monica, California in May 1997 and organized by the University of Southern California on tsunamigenic seafloor deformations, it had prophetically concluded that there was a need to develop better methods to identify tsunami generation from submarine slumping events versus slow earthquakes. Understanding this event will hopefully lead to the production of inundation maps for the north coast of PNG, similar to those in Hawaii and under development for some western States. Having access to inundation maps helps the local authorities locate schools, hospitals, fire-stations and other critical facilities

#### 9. LIST OF MEMBERS

Benson, USA  
 Borrero, USA  
 Jose Borrero, Univ. Southern Calif., USA  
 Willem de Lange, University of Waikato, NZ  
 Koji Fujima, National Defence Academy, JPN  
 Fumihiko Imamura, Tohoku University, JPN  
 Yoshiaki Kawata, Kyoto University, JPN  
 Masashi Matsuyama, CRIEPI, JPN  
 Hideo Matsutomi, Akita University, JPN

Jonathan Nott, James Cook University, Australia

Emil Okal, The Northwestern University, USA

Costas E. Synolakis, Univ. Southern Calif., USA

Tomoyuki Takahashi, Kyoto University, JPN

Yoshinobu Tsuji, Univ. Tokyo, JPN

#### 10. REFECERENCES

- Everingham, I. B. (1977) : Preliminary Catalogue of tsunamis for the New Guinea/Solomon islands region, 1768-1972, Australian Dept. of National Resources, Bureau of Mineral Resources, Geology and Geophysics, Report No. 180, 72p..
- Carey, S. W. (1935) : Preliminary notes on a recent earthquake in New Guinea, *Aust. Geogr.*, 2 (8), pp. 8-15.
- Davies, H.,L., (1990): Structure and evolution of the border region of New Guinea, in Carman G.J., and Carman, Z. (editor) *Petroleum Exploration in Papua New Guinea*, pp. 245-269.
- Imamura, F., D. Subandono, G. Watson, A. Moore, T. Takahashi, H. Matsutomi and R. Hidayat (1997) : Irian Jaya Earthquake and Tsunami causes serious damage, *EOS, Transactions, AGU*, Vol. 78, No. 19, p. 197 and pp. 201.
- IOC (1998) : Post-Tsunami survey field guide, Manual and Guides No. 37, UNESCO, 28p.
- Koshimura, S., L. Hamzah, and F. Imamura (1998) : Preliminary Report on earthquake and tsunami of the 1998 Papua New Guinea, Disaster Control Research Center, Tohoku University, 18p.
- Letz, H. (1985) : Seismizitat in Irian Jaya (west-Neuguinea), Indonesien, und ihre tektonische Bedeutung. *Berliner Geowissenschaftliche Abhandlungen, Reihe B/*

- Heft12, Verlag von Dietrich Reimer, Berlin.
- McCarthy, J. K. (1963): Patrol into yesterday, Canberra F. W. Cheshire, 156.
- Ripper, I.D. and H. Letz (1991): Distribution and origin of large earthquakes in the Papua New Guinea region, 1900-1989, Dept of Mining and Petroleum, Geological Survey, 77 p.
- Synolakis, C, F. Imamura, Y. Tsuji, H. Matsutomi, S. Tinti, B. Cook, Y. P. Chandra, and M. Usman (1995): Damage, conditions of East Java Tsunami of 1994 analyzed, EOS, Transactions, AGU, Vol. 76, No. 26, p. 257 and pp. 261-262.
- Yeh, H., F. Imamura, C. Synolakis, Y. Tsuji, P. Liu, S. Shi (1993): The Flores island tsunamis, EOS, Transactions, AGU, Vol. 74, No. 33, pp. 371-373,.



Table 5 Measured tsunami heights

Name of Place	Time (MON/DAY/HOUR:MIN)	tide correction (cm)	Measured Heights (no correction)	Corrected height (m)	Horizontal distance	Object/Marks	Accuracy	longitude	latitude
Malol-75	8/4/14:00	-0.3	6.75	6.75	999	broken branch	A	142.15	-3.075
Malol-75	8/4/14:00	-0.3	5.87	5.87	999	broken branch	A	142.15	-3.075
Malol-75	8/4/14:00	-0.3	4.85	4.85	999	broken branch	A	142.15	-3.075
Malol-74	8/4/13:26	-7.65	6.33	6.25	999	broken branch	A	142.154	-3.075
Malol-74	8/4/13:26	-7.65	6.6	6.52	999	broken branch	A	142.154	-3.075
Malol-72	8/4/11:24	-28.15	6.17	5.89	999	broken branch	A	142.158	-3.083
Malol-73	8/4/12:35	-20.65	8.14	7.93	999	broken branch	A	142.158	-3.083
Malol-73	8/4/12:35	-20.65	7.69	7.48	999	broken branch	A	142.158	-3.083
Malol-73	8/4/12:35	-20.65	8.14	7.93	999	broken branch	B	142.158	-3.083
Malol-73	8/4/12:35	-20.65	9.64	9.43	999	broken branch	B	142.158	-3.083
Malol-71	8/4/11:00	-30	6.16	5.86	999	broken branch	A	142.163	-3.083
Malol-72	8/4/11:24	-28.15	5.89	5.61	999	debris on branch	A	142.163	-3.083
Malol-72	8/4/11:24	-28.15	6.3	6.02	999	debris on branch	A	142.163	-3.083
Malol-71	8/4/10:30	-28.5	5.09	4.81	999	bark stripped from tree	A	142.167	-3.092
Malol-71	8/4/10:30	-28.5	5.55	5.27	999	bark stripped from tree	A	142.167	-3.092
Malol-?	8/4/9:55	-27	6.03	5.76	999	broken branch	A	142.171	-3.092
Malol-?	8/5/9:26	-14.15	5.55	5.41	999	broken branch	A	142.175	-3.092
Malol-Main Yeul	8/4/13:46	-3.975	3.97	3.93	999	bark stripped from tree	A	142.204	-3.1
Malol-Main Yeul	8/4/13:46	-3.975	3.18	3.14	999	bark stripped from tree	A	142.204	-3.1
Malol-	8/4/14:22	7.35	3.73	3.8	999	debris on	A	142.208	-3.1

## Appendix cont'd

Yiaml						coconut			
Malol-Yiaml	8/4/14:22	7.35	4.18	4.25	999	water mark on wall outside	A	142.208	-3.1
Malol-Yiaml	8/4/14:22	7.35	3.79	3.86	999	water mark on wall inside	A	142.208	-3.1
Malol-Tainapin	8/4/15:00	15.7	3.14	3.3	999	debris on road	A	142.208	-3.1
Malol-Arintin	8/4/16:48	36.15	2.24	2.6	999	debris on road	B	142.213	-3.108
Warapu	8/3/13:30	7.15	3.83	3.9	999	killed tree	A	142.071	-3.013
Warapu	8/3/14:45	23.6	6.06	6.3	999	?	A	142.066	-3.013
Warapu	8/3/13:55	14.3	7.81	7.95	999	?	A	142.07	-3.012
Warapu	8/3/13:30	7.15	5.03	5.1	999	killed tree	c	142.071	-3.013
Arop	8/3/16:15	36.05	10.8	11.16	999	?	B	142.086	-3.023
Arop	8/3/16:25	36.8	9.64	10.01	999	debris on road	B	142.086	-3.023
Arop	8/3/16:25	36.8	7.54	7.91	999	debris on road	B	142.086	-3.023
Arop	8/3/16:45	37.55	7.62	8	999	?	A	142.086	-3.023
Arop	8/3/16:45	37.55	8.56	8.94	999		B	142.086	-3.023
Arop	8/3/17:05	38.3	12.35	12.73	999	?	B	142.086	-3.023
Arop	8/3/17:05	38.3	7.59	7.97	999	Bucket on tree	B	142.086	-3.023
Arop	8/5/9:30	-14.15	11.87	11.73	999	broken branch	A	142.1	-3.033
Arop	8/5/9:50	-22.3	10.31	10.09	999	broken branch	A	142.1	-3.033
Arop	8/5/9:50	-22.3	15.25	15.03	999	broken branch	B	142.1	-3.033
Arop	8/5/10:15	-24.725	9.69	9.44	999	broken branch	A	142.106	-3.038
Arop	8/5/10:35	-27.15	11.22	10.95	999	broken branch	A	142.111	-3.041
Arop	8/5/10:50	-30.4	15.08	14.78	999	broken branch	A	142.114	-3.044
Arop	8/5/11:15	-32.575	14.69	14.36	999	?	A	142.121	-3.05
Arop	8/5/12:00	-34.3	7.48	7.14	999	broken branch	A	142.125	-3.054
Arop	8/5/12:20	-32.2	8.91	8.59	999	broken branch	A	142.133	-3.058
Arop	8/5/13:20	-23.7	7.82	7.58	999	?	A	142.136	-3.063
Arop	8/5/13:45	-18.25	10.39	10.21	999	broken branch	A	142.143	-3.068
Arop	8/5/13:55	-15	8.04	7.89	999	debris on tree	A	142.146	-3.069
Arop	8/3/11:00	-22	6.16	5.94	999	broken branch	A	142.163	-3.083
Malol	8/4/14:30	7.7	6.68	6.76	999	?	A	142.177	-3.092

## Appendix cont'd

Malol	8/4/14:10	2.37	7.36	7.38	999	?	A	142.18	-3.094
Malol	8/4/13:40	-5.2	10.44	10.39	999	?	A	142.184	-3.095
Malol	8/4/13:40	-5.2	11.94	11.89	999	?	B	142.184	-3.095
Malol	8/4/13:20	-10.1	9.45	9.35	999	?	A	142.187	-3.095
Malol	8/4/13:05	-15	7.63	7.48	999	?	A	142.189	-3.096
Malol	8/4/12:50	-12.55	7.7	7.57	999	debris on tree	A	142.193	-3.097
Malol	8/4/12:35	-20.65	6.25	6.04	999	debris on tree	A	142.194	-3.097
Malol	8/4/11:30	-28.15	5.93	5.65	999	rope on tree	A	142.198	-3.099
Malol	8/4/11:05	-30	8.34	8.04	999	killed tree	A	142.201	-3.099
Malol	8/4/10:40	-29	8.08	7.79	999	killed tree	A	142.203	-3.1
Malol	8/4/10:15	-27.75	10.19	9.91	999	cloth on tree	A	142.205	-3.1
Marok	8/6/10:50	-24.75	6.74	6.49	999	bakect on tree	A	142.271	-3.108
Marok	8/6/10:20	-17.1	7.56	7.39	999	broken branch	A	142.279	-3.125
Tepia	8/6/9:50	-8.72	4.6	4.51	999	broken branch	A	142.296	-3.125
Tepia	8/6/9:50	-8.72	4.33	4.24	999	debris	A	142.296	-3.125
Tepia	8/6/9:50	-8.72	3.99	3.9	999	debris	A	142.296	-3.125
Yokoi	8/6/9:10	4.4	7.16	7.2	999	witness about mark on wall	A	142.338	-3.133
Yokoi	8/6/9:10	4.4	3.36	3.4	999	broken branch	A	142.338	-3.133
Yokoi	8/6/9:40	-5.43	4.94	4.89	999	debris	A	142.338	-3.133
	8/5/14:30	-6.65	1.6	1.53	24.7m			141.884	-2.975
	8/5/13:50	-17.17	3.4	3.23	57m			141.946	-2.967
	8/5/13:20	-23.7	2.4	2.16	112.1m			141.969	-2.965
	8/5/12:30	-31.15	5.2	4.89	62m			141.986	-2.964
	8/5/10:45	-29.575	3	2.7	118.9m			141.993	-2.968
	8/5/9:30	-14.15	4.9	4.76	61.9m			141.994	-2.988
	8/5/17:00	34	5.2	5.54	26.2m			142.001	-2.97
	8/5/16:40	29.1	7.2	7.49	29m			142.006	-2.973
	8/5/17:50	41.5	6.9	7.32	24.0m			142.019	-2.977
	8/3/9:40	-23.57	3.5	3.26	153.9m inundati on			142.356	-3.149
	8/3/8:30	-14.85	3.4	3.25	157m inundati			142.359	-3.15

## Appendix cont'd

					on				
	8/6/14:08	-28	4.7	4.42	133.2m			142.395	-3.122
	8/6/13:40	-30.77	4.2	3.89	96m			142.395	-3.12
	8/6/12:20	-36.57	2.4	2.03	69.8m			142.397	-3.13
	8/6/13:09	-34.9	3.7	3.35	87.8m			142.403	-3.118
	8/4/15:20	20.37	6.4	6.6	199.6m			142.059	-3.005
	8/4/14:00	-0.3	6.9	6.9	87.8m			142.068	-3.009
	8/4/9:57	-27	11.3	11.03				142.079	-3.018
	8/3/16:15	36.05	10.8	11.16				142.086	-3.023
	8/3/17:30	37.5	12.35	12.73				142.09	-3.024
	8/4/16:49	36.87	9.6	9.97	42.1m			142.031	-2.985
	8/4/16:49	36.87	7.9	8.27	42.4m			142.031	-2.985
	8/2/7:00	-1.3	1.4	1.39	9.8m			143.171	-3.34
	8/2/15:50	35.3	0.5	0.85	5.2m			143.295	-3.239
	8/2/15:35	34.3	0.5	0.84	5.5m			143.298	-3.24
	8/2/15:00	33.3	0.3	0.63	3.4m			143.306	-3.244
	8/2/13:00	14.3	1.3	1.44	14.0m			143.337	-3.243
Waterstone	8/5/15:08	-12	1.52	1.4	999	eyewitness	A	141.339	-2.685
Ningrera	8/5/15:42	-2	1.95	1.93	999	eyewitness & debris	A	141.338	-2.713
Wutung-1	8/5/17:19	31	1.48	1.79	999	eyewitness & debris	A	140.02	-2.617
Wutung-2	8/5/17:19	39	2.7	3.09	999	eyewitness & debris	A	140.02	-2.617
Musa	8/5/18:34	48	2.19	2.67	999	eyewitness	A	140.3	-2.633



Photo 1 Survey team on the coast measuring tsunami heights after interview and checking marks



Photo 2 Installing the seismic records with ground acceralation sensors in three components





Photo 3 Coastal line nearby the Sissano lagoon taken from the aircraft. In the left of the photo, the water pool is created after the tsunami from Malol to Arop

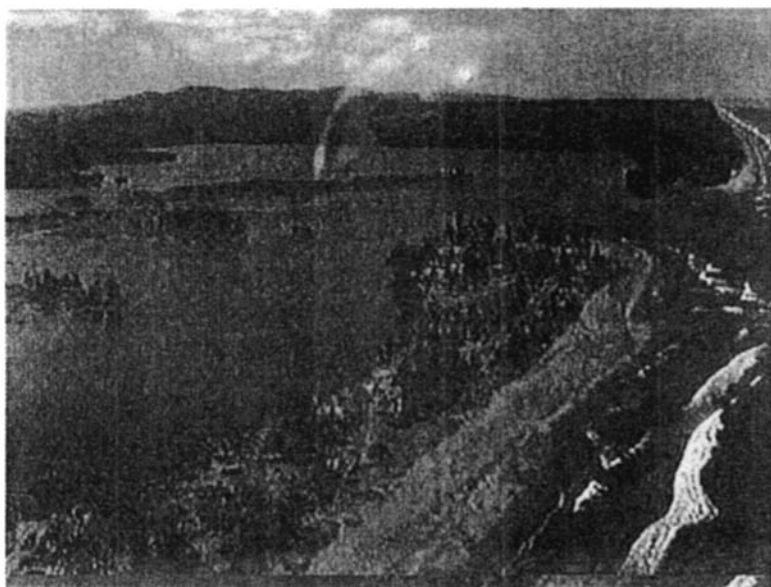


Photo 4 Mouth of the the Sissano lagoon where three villages were located before the tsunami attack



Photo 5 Scene of the damage by the tsunami at Arop village ; nothing are left and bending trees and glasses



Photo 6 A typical tsunami marks on trees which is a change color of leaves



Photo 7 Erosion of sand at the back side of sand bar, due to a strong current



Photo 8 Damaged houses in the left. A house with low floor was swept away. A sheltered house (right) with high floor remains without severe damage